PHYSICAL REVIEW D **82,** 103011 (2010)

Spectral representations of neutron-star equations of state

Lee Lindblom

Theoretical Astrophysics 350-17, California Institute of Technology, Pasadena, California 91125, USA

(Received 3 September 2010; published 18 November 2010)

Methods are developed for constructing spectral representations of cold (barotropic) neutron-star equations of state. These representations are faithful in the sense that every physical equation of state has a representation of this type and conversely every such representation satisfies the minimal thermodynamic stability criteria required of any physical equation of state. These spectral representations are also efficient, in the sense that only a few spectral coefficients are generally required to represent neutron-star equations of state quiet accurately. This accuracy and efficiency is illustrated by constructing spectral fits to a large collection of ''realistic'' neutron-star equations of state.

DOI: 10.1103/PhysRevD.82.103011 PACS numbers: 26.60.Kp, 26.60.−c, 26.60.Dd, 97.60.Jd

I. INTRODUCTION

The gravitational field of a neutron star compresses the material in its core to densities that exceed those inside normal atomic nuclei. The resulting matter is a mixture of free baryons (neutrons and protons), leptons (electrons and muons), and likely also smaller fractions of hyperons, mesons, or perhaps even free quarks. The basic thermodynamic relationship between the total energy density ϵ and the pressure p of this material is called its equation of state, $\epsilon = \epsilon(p)$, and is determined by the complicated microphysical interactions between the various particle species present in the mixture [1].

In addition to its dependence on the pressure, the energy density of a mixture also depends typically on the temperature and other quantities like the relative abundances of the different particle species. Thus there is no guarantee that a simple barotropic form, $\epsilon = \epsilon(p)$, applies to any, let alone universally to all, neutron-star matter. Yet there is reason to expect that a universal barotropic form might be an excellent approximation. Neutron stars are born when the cores of massive stars (and perhaps white dwarfs) become unstable and undergo gravitational collapse. Compression heats the material as it collapses, to temperatures that exceed the binding energies of all atomic nuclei. Neutron-star matter always begins therefore as a very hot plasma of free baryons and leptons, etc. This material is expected to evolve quickly to the lowest available energy state as it cools by neutrino and photon emission, and this fixes the relative abundances of the various particle species. The thermal energies of the particles fall rapidly below their Fermi levels, so the thermal contribution to the energy rapidly becomes negligible. The matter therefore is expected to evolve on a very short time scale to a state that is well described by a temperature independent barotropic equation of state. This paper develops more efficient ways to represent equations of state of this type.

The matter densities in the cores of neutron stars are well beyond the reach of current laboratory experiments. Heavy-ion scattering (including most recently those conducted at RHIC and LHC) provides a wealth of information about the interactions among the various particles expected to make up neutron-star matter. Unfortunately those experiments bear only indirectly on the properties of the equilibrium ground state, because the effective temperature of the nuclear matter in the experiments is quite high. Little insight is provided therefore into effects, like complicated many-body interactions, that might play a role only in states with low temperature and high density and pressure.

There has also been a significant effort over the past several decades to understand this material from a theoretical perspective: hundreds of papers devoted to modeling neutron-star matter have appeared in the literature. But the properties of this material are far outside the realm where the usual arsenal of theoretical tools was designed to work reliably, so it is not surprising that there is no consensus among theoreticians yet on the neutron-star equation of state. For example, the current models' predictions of the pressure at a given density still vary by about an order of magnitude [2].

Direct observations of neutron stars may be the most promising approach to understanding the properties of high-density nuclear matter. It is well known that the equation of state along with the gravitational field equations determine the observable macroscopic properties of neutron stars [3], and conversely that a complete knowledge of an appropriate set of macroscopic properties (e.g. masses and radii) determines the equation of state [4]. Studies of neutron-star models show that their macroscopic properties, like their masses and radii, vary widely even within the current ''realistic'' class of equations of state [2,5]. So it has long been recognized that accurate observations of the macroscopic properties of neutron stars will provide significant constraints on the nuclear equation of state. Unfortunately the needed observations are quite difficult to make. Masses of several dozen neutron stars have now been measured fairly accurately (see e.g. Ref. [6]), and these observations have ruled out large classes of very ''soft'' equation-of-state models. Only a

 © 2010 The American Physical Society

few radius measurements have been made however [7], and these are not reliable and accurate enough yet to make solid quantitative measurements of the equation of state itself possible.

There is reason to hope that more abundant and accurate measurements of both neutron-star masses and radii will become available, however. When the first accurate measurements are made, they are not likely to be numerous and accurate enough to determine the entire high-density portion of the neutron-star equation of state. Various attempts have been made, therefore, to find representations of equations of state that make their essential features depend on just a few parameters. One approach is to use the parameters that characterize the nuclear interaction models as a way to parametrize the equations of state constructed from them. These might include a number of microphysical parameters like the bulk nucleon incompressibility and symmetry energy parameters in models of the nucleon interaction potential [8], or the coupling constants and mixing angles in effective mean field theory descriptions [9]. Comparing the masses and radii of neutron stars based on these model equations of state should fix the values of the unknown nuclear interaction model parameters. This approach would clearly be ideal if a reliable and accurate microphysical model of neutron-star matter were known. Unfortunately there is no consensus that any of the existing nuclear-matter models are good enough yet to describe neutron-star matter accurately and reliably.

Another approach is to construct purely empirical fits rather than microphysics based models of the equation of state. The first attempts to do this [4,10] approximated the high-density part of the equation of state as a simple polytrope, i.e., an equation of state in which the pressure is proportional to a power of the density.[1] These first simple fits were shown to reproduce the central pressures and densities of neutron-star models based on realistic equations of state with about 15% accuracy [4]. This type of approximation can be improved by dividing the relevant range of pressures into a number of intervals, $p_0 < p_1 < \cdots < p_{\max}$, and fitting a different polytrope to the equation of state in each interval. Any level of accuracy can then be achieved by using a sufficiently large number of intervals. A number of authors have proposed using piecewise polytropes to approximate the high-density part of the neutron-star equation of state [2,10,11], and these approximations turn out to be quite efficient. Fits of the high-density parts of realistic neutron-star equations of state have been shown to achieve accuracies of a few percent for piecewise polytropes with only a small number of free parameters [2,10,11]. The most extensive study to date uses fits with four free parameters that give average errors of only a few percent for 34 realistic equations of state [2]. Other types of empirical fits to neutron-star equations of state have also been reported in the literature [12–15]. These provide high accuracy approximations of particular realistic equations of state (generally using 15 to 20 parameters to do this), and do not appear to have been intended as efficient ways to model large classes of equations of state.

This paper continues the effort to construct efficient empirical representations of realistic neutron-star equations of state. New methods are described here for constructing parametric representations based on spectral fits. Spectral representations are generalizations of the Fourier series used to represent periodic functions. It is shown in Sec. II that spectral representations can be constructed that are faithful, in the sense that every physical equation of state has such a representation and conversely that every such representation satisfies the basic thermodynamic stability conditions required of any equation of state. It is also shown in Sec. III that these spectral representations do a good job of representing the currently available realistic neutron-star equations of state. A suitably constructed two-parameter spectral representation is shown to be about as accurate as the most carefully studied four-parameter polytrope fits [2]. For smooth equations of state, the errors in the spectral fits decrease exponentially as the number of parameters is increased, while piecewise-polytrope fits generally decrease only quadratically. These spectral fits make it possible therefore to provide very accurate representations of the neutron-star equation of state using only a small number parameters. They should provide an important new tool for extracting the high-density equation of state from neutron-star observations.

II. SPECTRAL REPRESENTATIONS OF THE EQUATION OF STATE

Any equation of state, $\epsilon = \epsilon(p)$, can be represented in a "spectral" expansion, as linear combinations of basis functions $\Phi_k(p)$:

$$\epsilon(p) = \sum_k \epsilon_k \Phi_k(p). \tag{1}$$

Any complete set of functions, such as the Fourier basis functions or the Chebyshev polynomials, could be used as the Φ_k in these expansions. Equations of state are determined in such representations by their spectral coefficients, ϵ_k. Truncated versions of these expansions, in which only a finite number of terms are kept, provide approximate parametric representations of arbitrary equations of state: $\epsilon = \epsilon(p, \epsilon_k)$.

Physical equations of state must be non-negative, $\epsilon(p) \geq 0$, and monotonically increasing functions, $d\epsilon(p)/dp \geq 0$, to insure thermodynamic stability. Since almost all functions fail to satisfy these conditions, it

[1]The term relativistic polytrope is most commonly used for equations of state that satisfy $p \propto \rho^\Gamma$, where ρ is the conserved rest-mass density and Γ is the (constant) adiabatic index. It is also used (less commonly) for those satisfying $p \propto \epsilon^\gamma$ where ϵ is the total energy density and γ is a constant. The two definitions agree in the Newtonian limit.

follows that almost all choices of spectral coefficients, ϵ_k, in an expansion such as Eq. (1) represent functions that cannot be equations of state. Thus the spectral coefficients ϵ_k obtained by fitting to a physical equations of state are likely to produce a representation that violates basic thermodynamic stability. So unfortunately, representing an equation of state with a straightforward spectral expansion is not particularly useful.

Instead, faithful representations are needed, ones that ensure the positivity and monotonicity conditions for every choice of spectral coefficients. Methods of constructing faithful representations of the equation of state are presented in the following sections. Spectral representations of the standard form of the equation of state, in which the energy density is expressed as a function of the pressure $\epsilon = \epsilon(p)$, are presented in Sec. II A. For some applications it is more convenient to express the equation of state in terms of the relativistic enthalpy $\epsilon = \epsilon(h)$. Spectral representations of these enthalpy-based forms are given in Sec. II B.

A. Pressure-based forms

An equation of state $\epsilon(p)$ determines, and is determined by (up to an integration constant), the adiabatic index $\Gamma(p)$, defined by

$$\Gamma(p) = \frac{\epsilon + p}{p}\frac{dp}{d\epsilon}. \tag{2}$$

Given $\Gamma(p)$, the equation of state $\epsilon(p)$ is determined simply by integrating the first-order ordinary differential equation,

$$\frac{d\epsilon(p)}{dp} = \frac{\epsilon(p) + p}{p\Gamma(p)}. \tag{3}$$

The adiabatic index must be positive $\Gamma(p) > 0$ to ensure thermodynamic stability, but it need not be monotonic. Thus a larger class of functions represent possible physical adiabatic indices, and this makes it easier to represent equations of state through spectral expansions of $\Gamma(p)$. In particular, every physical equation of state can be represented by the following spectral expansion of the adiabatic index $\Gamma(p)$:

$$\Gamma(p) = \exp\Big[\sum_k \gamma_k \Phi_k(p)\Big]. \tag{4}$$

Conversely, every choice of γ_k (for which the series in this expansion converges) results in a positive adiabatic index, and thus an equation of state from Eq. (3), that satisfies the positivity and thermodynamic stability conditions. So this representation is faithful in the sense defined in Sec. II.

The construction of an explicit spectral representation of the equation of state requires a choice for the basis functions $\Phi_k(p)$. To that end, it is useful to define a dimensionless logarithmic pressure variable:

$$x = \log(p/p_0). \tag{5}$$

The constant p_0 is a scale factor, chosen here to be the minimum value of the pressure, $p_0 \le p$, in the domain where the spectral expansions are to be used. The following expansion of the adiabatic index $\Gamma(x)$ is found to be useful and effective:

$$\Gamma(x) = \exp\Big(\sum_k \gamma_k x^k\Big). \tag{6}$$

One advantage of this simple power-law basis is that the lowest order spectral coefficients γ_k have fairly simple physical interpretations. For example the lowest order coefficient, γ_0, is determined by the adiabatic index evaluated at the reference pressure $\gamma_0 = \log\Gamma(p_0)$. Similarly, the next coefficient, γ_1, determines the behavior of the adiabatic index, $\Gamma(p) \approx \Gamma(p_0)(p/p_0)^{\gamma_1}$ for pressures near p_0, i.e. for $x = \log(p/p_0) \ll 1$.

The power-law basis, $\Phi_k(x) = x^k$, has the advantage of simplicity. While it might be advantageous to choose another basis like the Chebyshev polynomials for some purposes, these advantages can only be fully exploited by using a knowledge of the exact range, $0 \le x \le x_{\max}$, and rescaling x in the optimal way. The additional information, like $x_{\max}$ for example, needed to do that will not be available *a priori* for the real neutron-star equation of state. So here the simple power-law basis is used, and fortunately this choice seems to work quite well.

Given an adiabatic index, $\Gamma(p)$, it is straightforward to determine the equation of state, $\epsilon(p)$, by integrating the ordinary differential equation, Eq. (3). The solutions and hence the equation of state can be reduced to quadratures:

$$\epsilon(p) = \frac{\epsilon_0}{\mu(p)} + \frac{1}{\mu(p)}\int_{p_0}^{p}\frac{\mu(p')}{\Gamma(p')}dp', \tag{7}$$

where $\mu(p)$ is defined as

$$\mu(p) = \exp\Big[-\int_{p_0}^{p}\frac{dp'}{p'\Gamma(p')}\Big], \tag{8}$$

and where $\epsilon_0 = \epsilon(p_0)$ is the constant of integration needed to fix the solution. This ϵ_0 is fixed in the fits performed in Sec. III by matching to a low density equation of state at the pressure, p_0 (i.e. at $x_0 = 0$), chosen to be a point somewhat below nuclear density.

The quadratures indicated in Eq. (7) cannot be done analytically for the expansion given in Eq. (6), so an explicit analytic expression for the equation of state is not available in this case. However, the integrands in these quadratures are analytic functions that can be integrated numerically very accurately and efficiently. Using Gaussian quadrature, for example, double precision accuracy can be achieved using about 10 points for each integral. So there is very little practical difference between having an explicit analytic expression for the equation of state, and the expression in Eq. (7) in terms of quadratures of explicit analytic functions.

It might be advantageous in some situations to construct spectral expansions for the equation of state using thermodynamic quantities other than $\Gamma(p)$. For example, the adiabatic sound speed, $v(p)$, defined by

$$v^2(p) = c^2\left[\frac{d\epsilon(p)}{dp}\right]^{-1}, \tag{9}$$

(where c is the speed of light) could be used to obtain the equation of state by integrating the simple ordinary differential equation,

$$\frac{d\epsilon(p)}{dp} = \frac{c^2}{v^2(p)}. \tag{10}$$

The thermodynamic stability condition, $0 \le v^2$, could be enforced in this case by constructing the following spectral expansion:

$$v^2(p) = c^2 \exp\left[\sum_k v_k \Phi_k(p)\right]. \tag{11}$$

Alternatively, it might be desirable to enforce both the thermodynamic stability condition and the "causality" conditions,[2] $0 \le v^2 \le c^2$, by constructing the spectral expansion in the following way:

$$v^2(p) = c^2\left\{1 + \exp\left[-\sum_k v_k \Phi_k(p)\right]\right\}^{-1}. \tag{12}$$

For the remainder of this paper, spectral representations of the equation of state will be based on the familiar adiabatic index $\Gamma(p)$. The discussion in Sec. III shows that $\Gamma(p)$ is a reasonably slowly varying function for realistic neutron-star equations of state, which can be represented fairly accurately using expansions having only a few terms. Using $\Gamma(p)$ for these expansions also allows us to make straightforward comparisons with published piecewise-polytrope approximations to the equation of state [2]. The accuracy and efficiency of these expansions in representing realistic neutron-star equations of state is explored in Sec. III.

B. Enthalpy-based forms

The spectral expansions of the standard representation of equation of state, $\epsilon = \epsilon(p)$, should be quite useful for many applications. For some applications, however, the standard representation, $\epsilon = \epsilon(p)$, is not ideal. For example, a useful form of the relativistic stellar structure equations [4] requires the equation of state to be expressed in terms of the relativistic enthalpy, h. For applications such as this, $\epsilon = \epsilon(p)$ must be rewritten as a pair of equations $\epsilon = \epsilon(h)$ and $p = p(h)$, where h is defined as

$$h(p) = \int_0^p \frac{dp'}{\epsilon(p') + p'}. \tag{13}$$

The needed expressions, $\epsilon = \epsilon(h)$ and $p = p(h)$, are constructed by inverting $h = h(p)$ from Eq. (13) to obtain $p = p(h)$, and composing the result with the standard equation of state, $\epsilon = \epsilon(p)$, to obtain $\epsilon(h) = \epsilon[p(h)]$.

The transformations needed to construct $\epsilon = \epsilon(h)$ and $p = p(h)$ are difficult to perform numerically in an efficient and accurate way. Therefore it may be preferable to construct a spectral expansion of the equation of state based directly on h. This can be done using the methods described above for the standard $\epsilon = \epsilon(p)$ representation. To do this a spectral expansion of the adiabatic index, considered now as a function of the enthalpy $\Gamma(h)$, must be defined. The scaled enthalpy variable $x = \log(h/h_0)$, is found to be useful, where h_0 is the lower bound on the enthalpy, $h_0 \le h$, in the domain where the spectral expansions are constructed. The expression for $\Gamma(x)$ given in Eq. (6) then provides a useful expansion for $\Gamma(h)$:

$$\Gamma(h) = \exp\left\{\sum_k \gamma_k\left[\log\left(\frac{h}{h_0}\right)\right]^k\right\}. \tag{14}$$

Next, the functions $p(h)$ and $\epsilon(h)$ are defined by the system of ordinary differential equations,

$$\frac{dp}{dh} = \epsilon + p, \tag{15}$$

$$\frac{d\epsilon}{dh} = \frac{(\epsilon + p)^2}{p\Gamma(h)}, \tag{16}$$

that follow from the definitions of h, Eq. (13), and Γ, Eq. (2). The general solution to these equations can be reduced to quadrature:

$$p(h) = p_0 \exp\left[\int_{h_0}^h \frac{e^{h'}dh'}{\tilde{\mu}(h')}\right], \tag{17}$$

$$\epsilon(h) = p(h)\frac{e^h - \tilde{\mu}(h)}{\tilde{\mu}(h)}, \tag{18}$$

where $\tilde{\mu}(h)$ is defined as

$$\tilde{\mu}(h) = \frac{p_0 e^{h_0}}{\epsilon_0 + p_0} + \int_{h_0}^h \frac{\Gamma(h') - 1}{\Gamma(h')} e^{h'}dh'. \tag{19}$$

The constants p_0 and ϵ_0 are defined by $p_0 = p(h_0)$ and $\epsilon_0 = \epsilon(h_0)$ respectively. While these quadratures cannot be done analytically for the spectral expansion defined in Eqs. (14), they can be done numerically very efficiently

[2]The condition $v^2 \le c^2$ only represents a true causality condition if the equation of state $\epsilon(p)$ describes both the time dependent and the equilibrium properties of the material. In neutron-star matter, various strong and weak nuclear interactions determine the relative abundances of the various particle species in the equilibrium state. Thus v^2 evaluated for the equilibrium equation of state only describes the sound propagation speed for low enough frequency waves that the material remains continuously in equilibrium. The condition $v^2 \le c^2$ may or may not represent a causality constraint therefore on sound waves with short enough wavelengths to be physically relevant in neutron stars.

and accurately using Gaussian quadrature, as in the standard equation of state case.

III. SPECTRAL FITS TO REALISTIC EQUATIONS OF STATE

The discussion in Sec. II shows how any equation of state can be represented by spectral expansions of the adiabatic index, like the one given in Eq. (6). When these expansions are truncated, keeping only a finite number of terms, they produce fits to the equation of state, $\epsilon_{\rm fit}(p)$, that are expected to converge to the exact $\epsilon(p)$ as the number of terms in the expansion increases. In analogy with Fourier series, the rate of convergence for these fits should be exponential for smooth equations of state, and power law for less than smooth cases. The smoothness of an equation of state is determined by the details of the microphysics that controls the properties of the material. The convergence rate of an expansion will be reduced therefore, from exponential to power law, when phase transitions or other nonsmooth transitions are present. The number of terms required to achieve a certain level of accuracy in $\epsilon_{\rm fit}(p)$, therefore, will depend on the smoothness and variability of the adiabatic index $\Gamma(p)$, and the suitability of the chosen spectral basis functions $\Phi_k(p)$.

The accuracy and practicality of spectral expansions for two forms of the equation of state, $\epsilon = \epsilon(p)$ and $\epsilon = \epsilon(h)$, are evaluated in this section by constructing fits to 34 realistic neutron-star equations of state. These spectral fits are based on finite spectral expansions of $\Gamma(p)$ and $\Gamma(h)$ respectively. The equations of state used for these fits are the same as those used by Read, Lackey, Owen, and Friedman [2] in their study of piecewise-polytrope approximations. These realistic equations of state are based on a

TABLE I. Spectral expansions of the standard $\epsilon = \epsilon(p)$ form of realistic neutron-star equations of state.

EOS	Δ_{P4}	Δ_{S2}	Δ_{S3}	Δ_{S4}	Δ_{S5}	γ_0	γ_1	γ_2	γ_3	p_0	ϵ_0/c^2	$x_{\rm max}$
PAL6	0.0076	0.0025	0.0014	0.0005	0.0001	0.8622	−0.0677	0.0181	−0.0017	3.01×10^{33}	2.03×10^{14}	5.79
SLy	0.0208	0.0076	0.0028	0.0010	0.0002	0.9865	0.1110	−0.0301	0.0022	1.64×10^{33}	2.05×10^{14}	6.73
AP1	0.0831	0.0552	0.0199	0.0098	0.0029	0.4132	0.5594	−0.1270	0.0085	1.16×10^{33}	2.02×10^{14}	7.38
AP2	0.0411	0.0236	0.0091	0.0033	0.0017	0.7065	0.2866	−0.0659	0.0047	1.34×10^{33}	2.02×10^{14}	7.27
AP3	0.0352	0.0204	0.0026	0.0011	0.0009	0.9214	0.2097	−0.0383	0.0019	1.51×10^{33}	2.02×10^{14}	6.87
AP4	0.0273	0.0194	0.0016	0.0015	0.0013	0.8651	0.1548	−0.0151	−0.0002	1.50×10^{33}	2.02×10^{14}	7.04
FPS	0.0120	0.0045	0.0037	0.0034	0.0021	1.1561	−0.0468	0.0081	−0.0010	1.19×10^{33}	2.04×10^{14}	7.04
WFF1	0.0320	0.0387	0.0067	0.0066	0.0062	0.6785	0.2626	−0.0215	−0.0008	1.14×10^{33}	2.04×10^{14}	7.48
WFF2	0.0342	0.0200	0.0077	0.0051	0.0041	0.8079	0.2680	−0.0558	0.0039	1.32×10^{33}	2.04×10^{14}	7.25
WFF3	0.0314	0.0081	0.0081	0.0060	0.0059	1.4126	−0.1797	0.0389	−0.0035	0.81×10^{33}	2.03×10^{14}	7.32
BBB2	0.1016	0.0283	0.0238	0.0167	0.0042	0.7390	0.4555	−0.1406	0.0121	1.37×10^{33}	2.05×10^{14}	6.97
BPAL12	0.0739	0.0138	0.0086	0.0043	0.0018	1.1081	−0.3078	0.0891	−0.0081	2.51×10^{33}	2.05×10^{14}	6.08
ENG	0.0527	0.0181	0.0168	0.0138	0.0118	0.9820	0.2716	−0.0862	0.0075	1.33×10^{33}	2.04×10^{14}	6.98
MPA1	0.0365	0.0223	0.0022	0.0022	0.0019	1.0215	0.1653	−0.0235	−0.0004	1.51×10^{33}	2.04×10^{14}	6.63
MS1	0.0581	0.0256	0.0052	0.0039	0.0004	0.9189	0.1432	0.0122	−0.0094	4.54×10^{33}	2.04×10^{14}	5.05
MS2	0.0155	0.0074	0.0013	0.0005	0.0001	0.9598	−0.0527	0.0091	−0.0035	4.10×10^{33}	2.04×10^{14}	4.77
MS1b	0.0206	0.0179	0.0058	0.0032	0.0004	1.2132	−0.0648	0.0561	−0.0111	3.18×10^{33}	2.03×10^{14}	5.40
PS	0.0568	0.0566	0.0294	0.0284	0.0182	1.3896	−0.8472	0.2636	−0.0218	5.49×10^{33}	2.05×10^{14}	4.77
GS1	0.0536	0.0762	0.0385	0.0333	0.0265	1.8662	−1.4266	0.4450	−0.0389	3.22×10^{33}	2.04×10^{14}	6.28
GS2	0.0416	0.0582	0.0427	0.0425	0.0294	1.4580	−0.7219	0.1828	−0.0117	4.06×10^{33}	2.04×10^{14}	4.99
BGN1H1	0.0435	0.0792	0.0460	0.0439	0.0328	1.3450	−0.0996	−0.0833	0.0161	2.30×10^{33}	2.05×10^{14}	6.40
GNH3	0.0092	0.0130	0.0090	0.0081	0.0057	1.0366	−0.0044	−0.0440	0.0075	3.77×10^{33}	2.06×10^{14}	5.26
H1	0.0226	0.0200	0.0117	0.0089	0.0069	1.0653	0.0362	−0.1098	0.0179	3.17×10^{33}	2.04×10^{14}	5.04
H2	0.0300	0.0181	0.0133	0.0072	0.0069	1.0743	0.2250	−0.2029	0.0290	2.96×10^{33}	2.04×10^{14}	4.98
H3	0.0308	0.0130	0.0109	0.0086	0.0066	1.1340	0.0925	−0.1303	0.0190	3.12×10^{33}	2.04×10^{14}	4.91
H4	0.0098	0.0098	0.0097	0.0069	0.0063	1.0526	0.1695	−0.1200	0.0150	3.16×10^{33}	2.04×10^{14}	5.21
H5	0.0214	0.0150	0.0126	0.0054	0.0054	1.0106	0.2765	−0.2011	0.0270	2.97×10^{33}	2.04×10^{14}	5.09
H6	0.0185	0.0137	0.0133	0.0130	0.0100	1.0650	−0.0196	−0.0474	0.0077	3.35×10^{33}	2.04×10^{14}	4.80
H7	0.0139	0.0132	0.0103	0.0059	0.0056	0.9582	0.1619	−0.1294	0.0177	3.19×10^{33}	2.04×10^{14}	5.22
PCL2	0.0227	0.0252	0.0121	0.0090	0.0075	1.0410	0.0173	−0.0904	0.0150	2.90×10^{33}	2.04×10^{14}	5.44
ALF1	0.0947	0.0669	0.0453	0.0369	0.0305	1.0143	−0.3102	0.1809	−0.0248	1.50×10^{33}	2.05×10^{14}	6.21
ALF2	0.0655	0.0629	0.0450	0.0256	0.0230	0.4613	1.5237	−0.5817	0.0571	1.50×10^{33}	2.05×10^{14}	5.79
ALF3	0.0371	0.0355	0.0139	0.0132	0.0131	0.8536	0.2405	−0.0743	0.0041	1.50×10^{33}	2.05×10^{14}	6.14
ALF4	0.0453	0.0652	0.0166	0.0089	0.0088	0.8806	0.0656	0.0765	−0.0177	1.50×10^{33}	2.05×10^{14}	5.97
Average	0.0383	0.0287	0.0149	0.0114	0.0085							

variety of different models for the composition of neutron-star matter, and a variety of different models for the interactions between the particle species present in the model material. Descriptions of these realistic equation of state models, and references to the original publications on each of these equations of state are given in Ref. [2], and are not repeated here. The individual equations of state are referred to here using the abbreviations used in Ref. [2], e.g. PAL6, APR1, BGN1H1, etc. The list of these equations of state are given in the first column of Table III of Ref. [2], and the first columns of Tables I and II in this paper.

Approximate equations of state, $\epsilon_{\rm fit}(p)$, have been constructed for each of the realistic neutron-star equations of state listed in Table I. These approximations are based on Eq. (7) with $\Gamma(x)$ determined by the spectral expansion in Eq. (6). The $\epsilon_{\rm fit}(p)$ constructed in this way depend on the pressure through the variable $x = \log(p/p_0)$, as well as the spectral coefficients γ_k: $\epsilon_{\rm fit} = \epsilon_{\rm fit}(x, \gamma_k)$. The optimal choice of spectral coefficients, γ_k, is made by minimizing the differences between $\epsilon_{\rm fit}(x_i, \gamma_k)$ and the exact $\epsilon_i = \epsilon(x_i)$ for a set of pressures, x_i, from the realistic neutron-star equation of state tables. These differences are measured by constructing the residual:

$$\Delta^2(\gamma_k) = \sum_{i=1}^{N} \frac{1}{N} \left\{ \log\left[\frac{\epsilon_{\rm fit}(x_i, \gamma_k)}{\epsilon_i} \right] \right\}^2, \tag{20}$$

where the sum is over all the pressures in the tabulated realistic equation of state in the range $p_0 \leq p_i \leq p_{\rm max}$. These are the pressures that may be present in the cores of

TABLE II. Spectral expansions of the $\epsilon = \epsilon(h)$ form of realistic neutron-star equations of state.

EOS	Δ_{S2}	Δ_{S3}	Δ_{S4}	Δ_{S5}	γ_0	γ_1	γ_2	γ_3	h_0	$x_{\rm max}$
PAL6	0.0032	0.0016	0.0005	0.0002	0.8608	−0.1509	0.0909	−0.0192	0.0405	2.62
SLy	0.0089	0.0035	0.0017	0.0006	1.0077	0.2084	−0.1266	0.0203	0.0314	3.22
AP1	0.0708	0.0331	0.0186	0.0081	0.5205	1.3288	−0.7804	0.1316	0.0276	3.31
AP2	0.0307	0.0139	0.0063	0.0034	0.7557	0.6423	−0.3586	0.0604	0.0287	3.34
AP3	0.0250	0.0054	0.0024	0.0015	0.9520	0.4691	−0.2109	0.0273	0.0298	3.40
AP4	0.0249	0.0030	0.0014	0.0014	0.8824	0.4064	−0.1405	0.0135	0.0297	3.41
FPS	0.0044	0.0041	0.0037	0.0018	1.1462	−0.1088	0.0432	−0.0106	0.0279	3.23
WFF1	0.0521	0.0105	0.0068	0.0064	0.7115	0.8263	−0.3258	0.0372	0.0273	3.53
WFF2	0.0267	0.0118	0.0070	0.0037	0.8527	0.6162	−0.3135	0.0512	0.0285	3.48
WFF3	0.0109	0.0101	0.0058	0.0054	1.3660	−0.4236	0.2293	−0.0469	0.0253	3.30
BBB2	0.0318	0.0277	0.0210	0.0089	0.8447	0.8101	−0.5808	0.1120	0.0297	3.24
BPAL12	0.0168	0.0097	0.0048	0.0022	1.0847	−0.6537	0.4289	−0.0874	0.0373	2.73
ENG	0.0195	0.0179	0.0142	0.0109	1.0426	0.4716	−0.3353	0.0632	0.0286	3.39
MPA1	0.0251	0.0032	0.0030	0.0022	1.0523	0.3546	−0.1356	0.0074	0.0297	3.33
MS1	0.0277	0.0055	0.0035	0.0003	0.9340	0.2231	0.0718	−0.0642	0.0485	2.73
MS2	0.0096	0.0021	0.0003	0.0001	0.9680	−0.1326	0.0786	−0.0360	0.0367	2.56
MS1b	0.0192	0.0062	0.0029	0.0003	1.2148	−0.1255	0.1959	−0.0700	0.0403	2.92
PS	0.0624	0.0298	0.0298	0.0166	1.3064	−1.2479	0.5534	−0.0186	0.0571	2.26
GS1	0.0889	0.0383	0.0377	0.0249	1.7649	−1.9609	0.8871	−0.0942	0.0265	3.22
GS2	0.0603	0.0437	0.0433	0.0314	1.2562	−0.4936	−0.1125	0.1051	0.0362	2.61
BGN1H1	0.0868	0.0495	0.0439	0.0403	1.1915	0.2463	−0.7222	0.2300	0.0356	2.97
GNH3	0.0135	0.0093	0.0081	0.0057	1.0236	0.0297	−0.2197	0.0742	0.0482	2.53
H1	0.0200	0.0122	0.0084	0.0071	1.0365	0.1735	−0.5519	0.1790	0.0406	2.39
H2	0.0173	0.0136	0.0067	0.0067	1.0666	0.4639	−0.8300	0.2393	0.0391	2.41
H3	0.0124	0.0109	0.0082	0.0068	1.1204	0.2084	−0.5285	0.1519	0.0402	2.42
H4	0.0103	0.0100	0.0066	0.0066	1.0070	0.4040	−0.3709	0.0696	0.0223	3.18
H5	0.0137	0.0134	0.0059	0.0049	0.9614	0.6257	−0.6459	0.1371	0.0233	2.96
H6	0.0137	0.0135	0.0129	0.0113	1.0182	0.1483	−0.2638	0.0628	0.0263	2.79
H7	0.0123	0.0112	0.0057	0.0057	0.9147	0.4331	−0.4779	0.1064	0.0254	2.94
PCL2	0.0265	0.0130	0.0086	0.0077	1.0127	0.1289	−0.4822	0.1616	0.0389	2.52
ALF1	0.0731	0.0475	0.0400	0.0283	0.9349	−0.3810	0.6697	−0.2305	0.0305	2.75
ALF2	0.0692	0.0490	0.0276	0.0178	0.7100	2.6577	−2.2438	0.4712	0.0305	2.83
ALF3	0.0386	0.0149	0.0140	0.0134	0.8987	0.4588	−0.3533	0.0489	0.0305	2.73
ALF4	0.0708	0.0135	0.0099	0.0094	0.8705	0.4469	0.0284	−0.0914	0.0305	2.83
Average	0.0323	0.0166	0.0124	0.0089						

neutron stars where the equation of state is not well known: p_0 is the pressure where the baryon density is $\rho_0 = 2 \times 10^{14}$ g/cm^3, and $p_{\max}$ is the central pressure of the maximum-mass nonrotating neutron-star model for the particular equation of state. The constants p_0, $x_{\max} = \log(p_{\max}/p_0)$, and the total energy density, $\epsilon_0 = \epsilon(p_0)$, are given (in centimeter-gram-second units) in the last three columns of Table I for each of the realistic equations of state. This range of pressures coincides with the range used by Read, Lackey, Owen, and Friedman [2] to construct their piecewise-polytrope fits. Using the same range of pressures here makes comparison with their work more straightforward.

The spectral coefficients, γ_k, that determine the particular $\epsilon_{\rm fit}(x, \gamma_k)$ are chosen to minimize the residual $\Delta(\gamma_k)$ for each realistic equation of state. The minimization process was carried out with an algorithm based on the Levenberg-Marquardt method [16], starting with initial estimates, $\gamma_0 = 1$ and $\gamma_k = 0$ for $k \geq 1$. Approximate $\epsilon_{\rm fit}$ were constructed in this way for expansions containing 2, 3, 4, and 5 spectral basis functions. The minimum values of the residuals, Δ_{S2}, Δ_{S3}, Δ_{S4}, and Δ_{S5}, for these cases are listed for each equation of state in Table I. The average values of these minimum residuals decrease from about 2.9% for the 2-parameter fits, to about 0.9% for the 5-parameter fits. For comparison the residuals Δ_{P4} for the 4-parameter piecewise-polytrope fits of Reid, Lackey, Owen, and Friedman [2] are also given in Table I for each equation of state.[3] The values of the residuals, Δ_{S2}, Δ_{S3}, Δ_{S4}, Δ_{S5}, and Δ_{P4}, are also shown graphically in Fig. 1. Points along the horizontal axis in Fig. 1 represent the different realistic equations of state in the order listed in Table I. These results show that the spectral fits are convergent, and do a fairly good job of approximating this collection of realistic equations of state. The 2-parameter spectral fits have smaller residuals than the 4-parameter piecewise-polytrope fits for most of these equations of state. Also listed in Table I are the optimal values of the spectral coefficients, γ_0, γ_1, γ_2, and γ_3, for the 4-parameter spectral approximation to each equation of state. These values, together with the tabulated constants ϵ_0 and p_0 can be used to reconstruct the complete 4-parameter spectral fits for $\epsilon(p)$, using Eqs. (6) and (7).

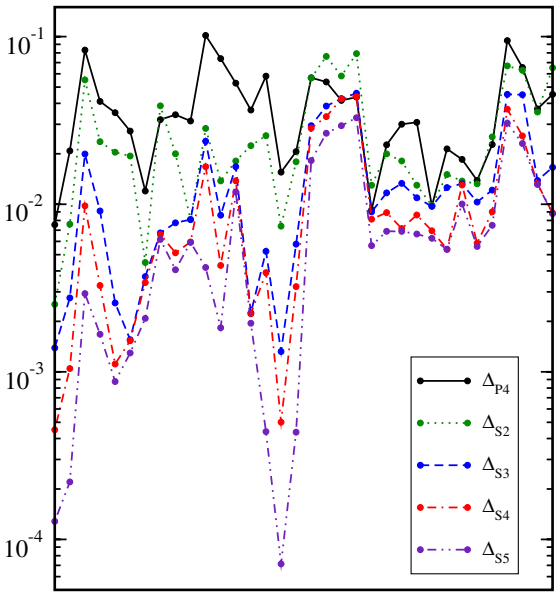

FIG. 1 (color online). Residuals Δ_{Sk} are illustrated for several spectral fits and for the polynomial fit Δ_{P4} for each of the realistic equation of state models, which are represented as points along the horizontal axis in this figure. These residuals are for standard pressure-based representations of the equation of state, $\epsilon = \epsilon(p)$, which are also given in Table I.

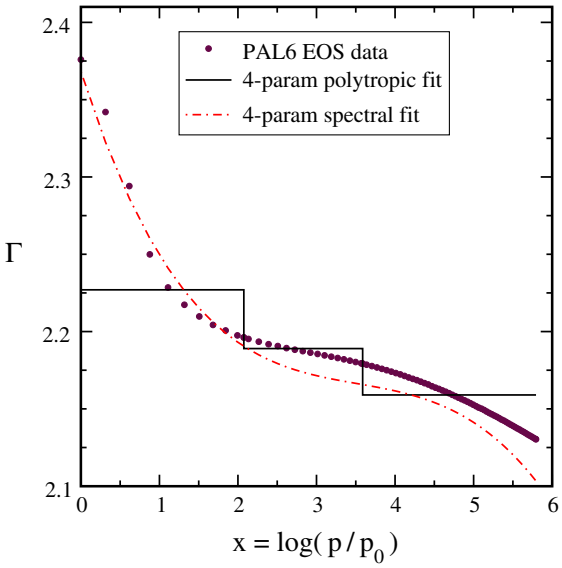

FIG. 2 (color online). Adiabatic index as a function of pressure, $\Gamma(x)$, for various fits to the PAL6 equation of state.

Three equations of state have been chosen from the complete set to illustrate in more detail the accuracy of the fits. These three cases are equation of state PAL6 having the highest accuracy spectral fits, APR1 having spectral fits with average accuracy, and BGN1H1 having the lowest accuracy spectral fits. Figures 2–4 show the adiabatic index $\Gamma(x)$ computed directly from the tabulated equations of state, the 4-parameter spectral fit to the adiabatic index, and the 4-parameter piecewise-polytrope fit for each equation of state (EOS). From these figures it is clear

[3]The residuals reported in Table III of Ref. [2] differ from the Δ_{P4} residual listed in Table I in two ways. The first difference is the residuals reported in Ref. [2] are evaluated using base-10 logarithms, rather than the natural logarithms used here. This difference makes the Ref. [2] residuals smaller by the factor $\log_{10} e \approx 2.3$. The second difference is that Δ_{P4} reported here measures the accuracy of the piecewise-polytrope fits for $\epsilon(p)$, while the residuals reported in Ref. [2] measure the accuracy of those fits for $p(\rho)$, where ρ is the baryon density of the material.

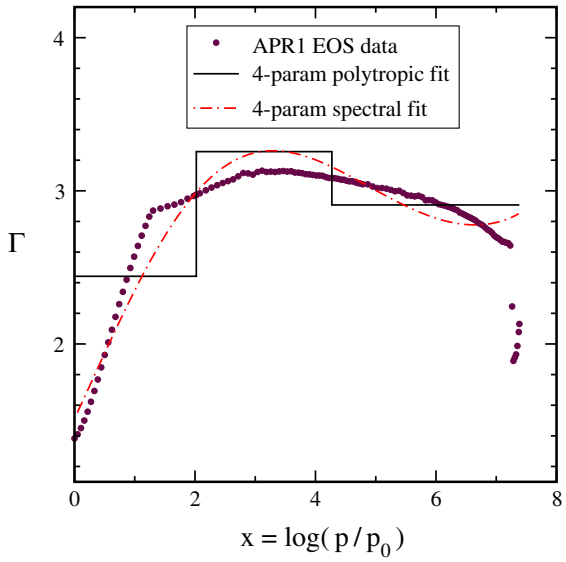

FIG. 3 (color online). Adiabatic index as a function of pressure, $\Gamma(x)$, for various fits to the APR1 equation of state.

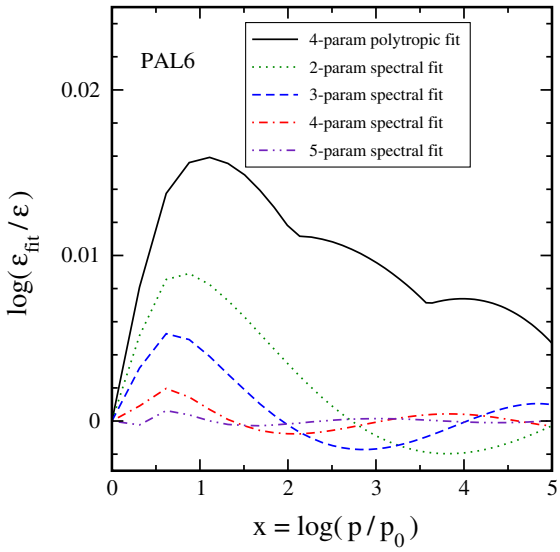

FIG. 5 (color online). Ratios between various fits, $\epsilon_{\rm fit}(x)$, and the exact PAL6 equation of state, $\epsilon(x)$. Note that $\log(\epsilon_{\rm fit}/\epsilon) \approx (\epsilon_{\rm fit} - \epsilon)/\epsilon$ measures the fractional error of the fit.

that the smoother equations of state, like PAL6, have the highest accuracy fits, while the equations of state with a sharp phase transition, like BGN1H1, have the lowest accuracy fits. Figures 5–7 illustrate the errors in the various fits to the equation of state $\epsilon(x)$ for these three example equations of state. These errors are illustrated as graphs of $\log(\epsilon_{\rm fit}/\epsilon) \approx (\epsilon_{\rm fit} - \epsilon)/\epsilon$, as functions of the pressure variable $x = \log(p/p_0)$. These figures show that the spectral fits are much more accurate than the 4-parameter piecewise-polytrope fit for the smooth and average equations of state, PAL6 and APR1. The spectral fits have about the same accuracy as the piecewise-polytrope fit for equation of state BGN1H1 which has a strong phase transition. Figures 5–7 also illustrate in a visual way the convergence of the spectral fits as the number of basis functions is increased.

The enthalpy-based representation of the equation of state, $\epsilon = \epsilon(h)$ and $p = p(h)$, is more useful for certain purposes. It is helpful to understand, therefore, whether the spectral fits for this representation, Eqs. (14)–(19), are as accurate and effective as those for the standard $\epsilon = \epsilon(p)$ representation. So approximate equations of state, $\epsilon_{\rm fit}(h)$, have been constructed for the same set of 34 realistic neutron-star equations of state described in Ref. [2]. As before these fits were made by adjusting the values of the spectral coefficients γ_k defined in Eq. (14), to minimize the

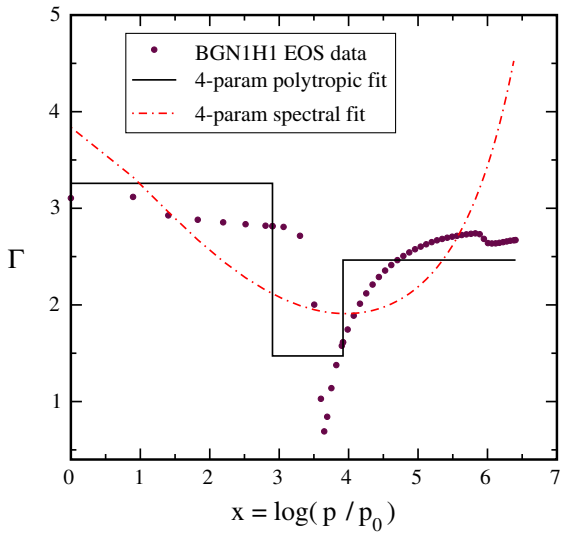

FIG. 4 (color online). Adiabatic index as a function of pressure, $\Gamma(x)$, for various fits to the BGN1H1 equation of state.

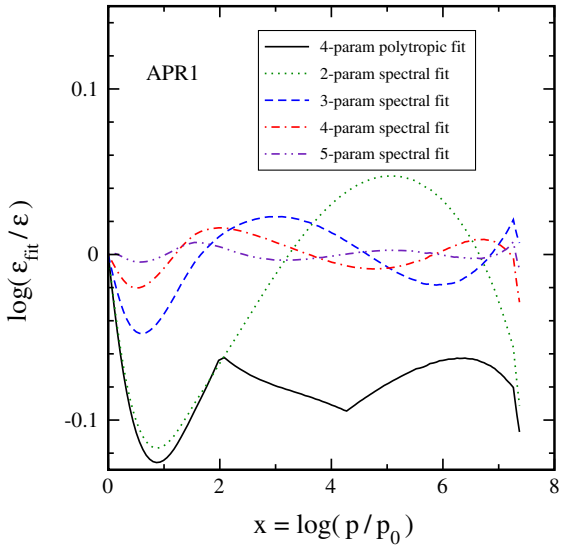

FIG. 6 (color online). Ratios between various fits, $\epsilon_{\rm fit}(x)$, and the exact APR1 equation of state, $\epsilon(x)$. Note that $\log(\epsilon_{\rm fit}/\epsilon) \approx (\epsilon_{\rm fit} - \epsilon)/\epsilon$ measures the fractional error of the fit.

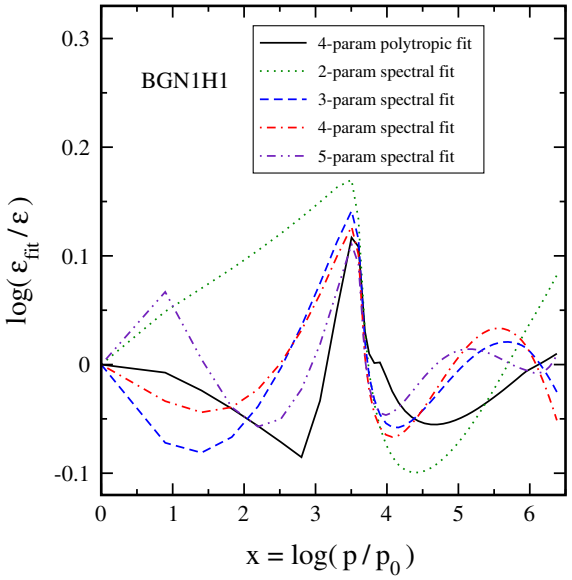

FIG. 7 (color online). Ratios between various fits, $\epsilon_{\rm fit}(x)$, and the exact BGN1H1 equation of state, $\epsilon(x)$. Note that $\log(\epsilon_{\rm fit}/\epsilon) \approx (\epsilon_{\rm fit} - \epsilon)/\epsilon$ measures the fractional error of the fit.

residual $\Delta(\gamma_k)$ defined in (20). The only differences between this and the standard case are: The variable $x = \log(h/h_0)$ is chosen here to be an enthalpy variable, and the functions $\epsilon(h, \gamma_k)$ and $p(h, \gamma_k)$ are determined here with Eqs. (17)–(19). Table II lists each equation of state, along with the residuals, Δ_{S2}, Δ_{S3}, Δ_{S4}, and Δ_{S5}, for the spectral fits having 2, 3, 4, and 5 nonzero spectral coefficients. The values of the residuals, Δ_{S2}, Δ_{S3}, Δ_{S4}, Δ_{S5}, and Δ_{P4}, are also show graphically in Fig. 8 for these enthalpy-based fits. Table II also lists the coefficients, γ_0, γ_1, γ_2, and γ_3 for the 4-parameter spectral fit. Finally, Table II contains information about the enthalpy variables, h_0 and $x_{\rm max} = \log(h_{\rm max}/h_0)$, for each equation of state. The quantity h_0 is the enthalpy for which $\epsilon_0 = \epsilon(h_0)$ and $p_0 = p(h_0)$ whose values are listed in Table I, and $h_{\rm max}$ is the value for which $p_{\rm max} = p(h_{\rm max})$. These results show that the spectral expansions of the enthalpy-based representation of the equation of state are very comparable to the standard expansions.

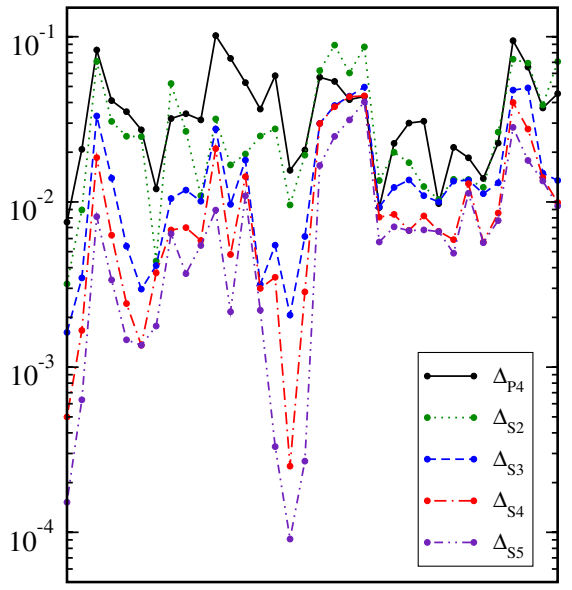

FIG. 8 (color online). Residuals Δ_{Sk} are illustrated for several spectral fits and for the polynomial fit Δ_{P4} for each of the realistic equation of state models, which are represented as points along the horizontal axis in this figure. These residuals are for enthalpy-based representations of the equation of state, $\epsilon = \epsilon(h)$, which are also given in Table II.

IV. DISCUSSION

The spectral fits constructed here were designed to explore how accurately the real neutron-star equation of state might be determined once the first few accurate neutron-star mass-radius measurements become available. These fits could be improved for equations of state with phase transitions by using separate spectral fits above and below the phase-transition pressure. These piecewise spectral fits could eliminate Gibbs phenomena errors, but would require significantly more (roughly double the number of) parameters. Measuring this larger number of parameters from neutron-star observations would therefore require a much larger number of accurate mass-radius determinations. A systematic study of the relative accuracy of single versus piecewise spectral expansions (with the same total number of free parameters) will therefore be delayed until more neutron-star measurements become available.

The fits constructed here show that spectral representations of the various realistic neutron-star equations of state are remarkably accurate, even when the number of basis functions used in the spectral expansion is rather small. Such expansions provide an attractive alternative to the piecewise-polytrope approximations for a variety of current realistic models of the equation of state. If the real neutron-star equation of state is relatively smooth, then these spectral expansions will provide an extremely efficient way to represent it. And remarkably, even if the neutron-star equation of state has a phase transition, these spectral fits do about as well as the piecewise-polytrope fits with the same number of free parameters.

ACKNOWLEDGMENTS

I thank Benjamin Owen, Benjamin Lackey, John Friedman, and Chris Vuille for helpful discussions about their work, B. O., B. L., and C. V. for useful comments on an earlier draft of this paper, and B. L and J. F. for providing tables of the various realistic equations of state used here. This research was supported in part by a grant from the Sherman Fairchild Foundation, by NSF Grant No. PHY-0601459, and by NASA Grant No. NNX09AF97G.

[1] S. L. Shapiro and S. A. Teukolsky, *Black Holes, White Dwarfs, and Neutron Stars* (Wiley, New York, 1983).
[2] J. S. Read, B. D. Lackey, B. J. Owen, and J. L. Friedman, Phys. Rev. D **79**, 124032 (2009).
[3] J. R. Oppenheimer and G. M. Volkoff, Phys. Rev. **55**, 374 (1939).
[4] L. Lindblom, Astrophys. J. **398**, 569 (1992).
[5] W. D. Arnett and R. L. Bowers, Astrophys. J. Suppl. Ser. **33**, 415 (1977).
[6] J. M. Lattimer and M. Prakash, Phys. Rep. **442**, 109 (2007).
[7] A. W. Steiner, J. M. Lattimer, and E. F. Brown, Astrophys. J. **722**, 33 (2010).
[8] M. Prakash, T. L. Ainsworth, and J. M. Lattimer, Phys. Rev. Lett. **61**, 2518 (1988).
[9] N. K. Glendenning, Astrophys. J. **293**, 470 (1985).
[10] C. Vuille, arXiv:0812.3828.
[11] C. Vuille and J. Ipser, in *Eighth Canadian Conference on General Relativity and Relativistic Astrophysics*, edited by C. P. Burgess and R. C. Meyers, AIP Conf. Proc. No. 493 (AIP, New York, 1999).
[12] P. Haensel and A. Y. Potekhin, Astron. Astrophys. **428**, 191 (2004).
[13] M. Shibata, K. Taniguchi, and K. Uryu, Phys. Rev. D **71**, 084021 (2005).
[14] M. Shibata and K. Taniguchi, Phys. Rev. D **73**, 064027 (2006).
[15] J. L. Zdunik, M. Bejger, P. Haensel, and E. Gourgoulhon, Astron. Astrophys. **450**, 747 (2006).
[16] W. H. Press, S. A. Teukolsky, W. T. Vetterling, and B. P. Flannery, *Numerical Recipes in FORTRAN* (Cambridge University Press, Cambridge, England, 1992), 2nd ed.